Topological Analysis of the Electron Localization Function (ELF) Applied to the Electrophilic Aromatic Substitution

Franck Fuster, Alain Sevin, and Bernard Silvi*

Laboratoire de Chimie Théorique (UMR-CNRS 7616), Université Pierre et Marie Curie, 4 Place Jussieu, 75252-Paris cédex, France

Received: August 5, 1999; In Final Form: October 20, 1999

The topological analysis of the electron localization function ELF provides a partition of the molecular space into basins of attractors which have a clear chemical signification. The hierarchy of these basins is given by the bifurcation of the localization domains. In the case of π-donor substituents (OH, NH_2, F, CH_3, C_6H_5, Cl), the aromatic domain is first opened close to the substituted carbon and then in the vicinity of the *meta* carbon; whereas for attractor substituents (CN, CHO, NO_2, CF_3 and CCl_3), it is first opened in the *ortho* and *para* positions. The orienting effects of the electrophilic substitutions are correlated with these bifurcations. The experimental favored positions always correspond to the locally electronegative carbons (i.e., those which keep their shell structure at the higher ELF values). This suggests that the local Pauli repulsion plays a noticeable role in the orienting effects which are complementary to the charge transfer effect involved in standard quantum chemical pictures.

1. Introduction

Since the early work of Kekulé, aromatic compounds have played a major role in the development of chemical concepts. Though their reactivity, and more especially the so-called electrophilic substitution, has been widely studied and empirically classified according to Holleman's rules[1−4] as early as 1925, the progressive appearance of a rationale has followed the progress of the electronic theory of molecules. The close interplay between experiment and theory is illustrated by the fundamental contribution of Hückel[5−7] in the 1930s and Wheland[8] and Ingold[9] in the 1950s and then by the classical MO approach, illustrated by the classical works of Coulson,[10] Streitwieser,[11] Salem,[12] and Dewar[13] in the 1960s and Epiotis[14−17] in the 1970s.

Recently, new proposals that constitute a revival of the topic have appeared on the grounds of Bader's atoms in molecules theory[18−20] as well as of the molecular electrostatic potential.[21] Even more recently, many applications of the Becke and Edgecombe's electron localization function (ELF)[22] have proven to allow for an efficient description of chemical bonding in stable molecules and short-lived intermediates.

We propose here an investigation of Holleman's rules in electrophilic aromatic substitution using ELF methodology. Our goal is dual. First, we hope to illustrate constructive new concepts which, second, we will use as a pretext to comfort ELF results with firmly established evidence.

Prior to the detailed account of our study, it is worth recalling the general framework which is used in the investigation of electrophilic substitution mechanism. Actually, two different kinds of approaches are often made. The first one considers the electronic properties of a suitably substituted aromatic ring and deduces the preferential site of attack by the incoming substituent. This method may be referred to as "reactant like". The second considers the relative stability of *ortho*, *meta*, and *para* Wheland cationic intermediates and thus deduces the resulting regioselectivity. The latter approach is typically "intermediate like", and upon the assumption that the transition state closely resembles the intermediate species, it no longer refers to the isolated aromatic entity. As Bader's, our approach is only related to the first type of argument. The article is organized as follows: after a brief methodological introduction, the role of various *ortho*−*para* and *meta* orienting substituents on benzene is investigated in order to establish in which way the topology of the ELF function accounts for the Holleman's rules. The analysis is then generalized to multiple substitutions and to polyaromatic substituted hydrocarbons.

2. Methodology

The quantum mechanical calculations have been performed with the standard 6-31G** basis set[29−31] at the Hartree−Fock and hybrid Hartree−Fock density functional Becke3LYP[32−35] levels using the Gaussian94 package.[36] The aim of the topological analysis of ELF is to provide a mathematical model of the Lewis representation. The simplest mathematical structure enabling the partition of the molecular space and accounting for its evolution upon the variation of parameters (such as the nuclear coordinates within the Born−Oppenheimer approximation) is a gradient dynamical system. A gradient dynamical system is the gradient vector field of a scalar, continuous, derivable function named the potential function. The potential function carries the physical (or chemical) information. For example, the gradient field of the electron density distribution yields a partition into atomic basins.[18] Many studies have shown that the electron localization function (ELF) of Becke and Edgecombe[22] yields a faithful description of the bonding consistent with the Lewis approach[25−28,37−41] as well as it accounts for its evolution during reactive processes.[42−45]

The Gaussian wfn output was then treated with the TopMod package written in our group.[46] The latter program first calculates the ELF, over the molecular space, according to its definition

$$\eta(\mathbf{r}) = \frac{1}{1 + \left(\frac{D^{\sigma}(\mathbf{r})}{D_h^{\sigma}(\mathbf{r})}\right)^2} \qquad (1)$$

where D^{σ} stands for the excess local kinetic energy due to the

* E-mail: silvi@lct.jussieu.fr. Fax: +033 01 4427 4053.

10.1021/jp992783k CCC: $19.00
Published on Web 01/07/2000

Pauli restriction,[23] i.e., the difference between the definite positive kinetic energy density $T_s(\mathbf{r})$ of the actual fermionic system and that of the von Weizsäcker kinetic energy functional $T_{uW}(\mathbf{r})$.[47] If the wave function is written as a single determinant, D^σ is expressed in terms of orbital contributions:

$$D^\sigma(\mathbf{r}) = \frac{1}{2}\sum_i |\nabla\phi_i(\mathbf{r})|^2 - \frac{1}{8}\frac{|\nabla\rho(\mathbf{r})|^2}{\rho(\mathbf{r})} \quad (2)$$

D_h^σ is the kinetic energy of the electron gas having the same density:

$$D_h^\sigma(\mathbf{r}) = C_F\rho(\mathbf{r})^{5/3} \quad (3)$$

where C_F is the Fermi constant. Where electrons are alone, or form pairs of antiparallel spins, the Pauli principle has little influence on their behavior and the excess local kinetic energy has a low value and, therefore, ELF is close to 1, whereas at the boundaries between such regions the probability of finding parallel spin electrons close together is rather high and the excess local kinetic energy has a large value and ELF is small. The topological analysis is carried out in order to partition the molecular space into basins of attractors denoted by Ω_A. Each basin is characterized by an attractor which is a local maximum of ELF. One distinguishes core basins, labeled $C(X_i)$, centered on atoms X_i, and valence basins, between atoms, labeled $V(X_i, X_j, ...)$. For each basin one defines its synaptic order which is the number of core basins that it is connected to. Integration of the electronic density over the Ω_A basin yields its population. The dependence of basin populations upon basis set and correlation effects is consistent with the chemical intuition. On one hand, the addition of polarization functions increases the disynaptic (bonding) basin populations at the expense of the monosynaptic ones (lone pairs), and correlatively the dissociation energy and the stretching force constants are enhanced. On the other hand, correlation yields the opposite trend in agreement with the lowering of the force constants.[39] Moreover, there is an overall very good agreement between the MP2 and DFT values[38,39] though the former method appears to be much more basis set dependent. In the systems investigated here, the electron correlation is not expected to play an important role with respect to the electronic state or to the structure; moreover it has been shown that the properties related to the ELF topological analysis are almost converged with a polarized split-valence basis set.[28]

As it will be seen in the next sections, the value of the ELF function at some particular critical points is of a great importance in the present study. These critical points are located by a steepest ascent search which uses the analytical derivatives of the norm of the ELF gradient.

Graphical representations of the bonding are obtained by plotting isosurfaces of the localization function which delimit volumes within which the Pauli repulsion is rather weak. These latter, the localization domains, are called irreducible when they contain one and only one attractor.

3. *f*-Localization Domains in the Model Study of Benzene

These domains define the bodies limited by a given isosurface $\eta(r) = f$, enclosing points for which $\eta(r) > f$. They are said to be reducible when they contain more than one attractor. For a low value of ELF there exists only one reducible localization domain which contains all the molecule population. Upon progressive increase of ELF, the overall isosurface splits into reducible valence and irreducible core domains. Thus, there exists a

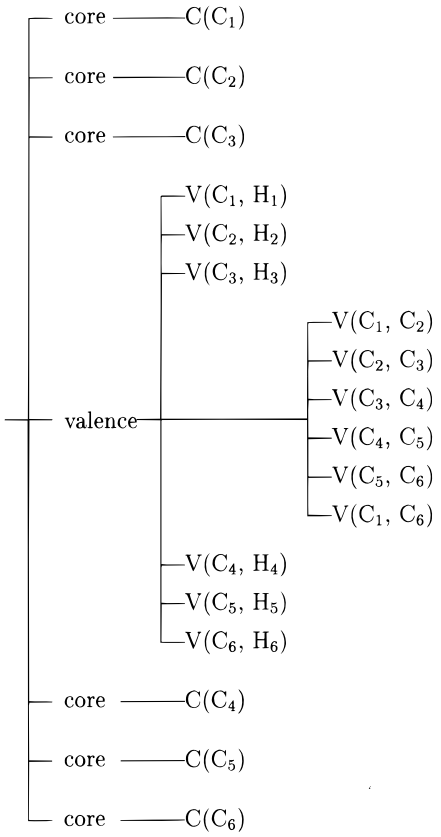

Figure 1. Localization domain reduction tree-diagram of benzene.

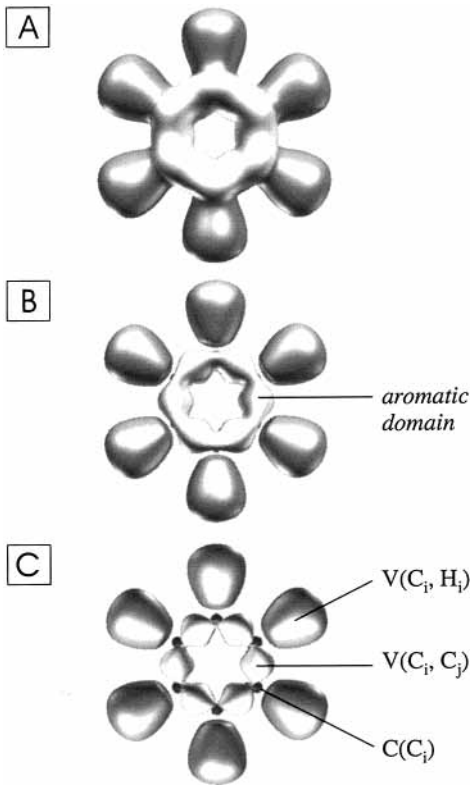

Figure 2. ELF isosurface of benzene. Value of ELF is equal to (A) 0.5, (B) 0.64, and (C) 0.65. The gray scale code used for the localization domain is as follows: core, black; valence protonated, gray; valence disynaptic, light gray. This figure, presented here in black and white, is available in color on the World Wide Web in Supporting Information. Color code: magenta = core, red = valence monosynaptic, green = valence disynaptic.

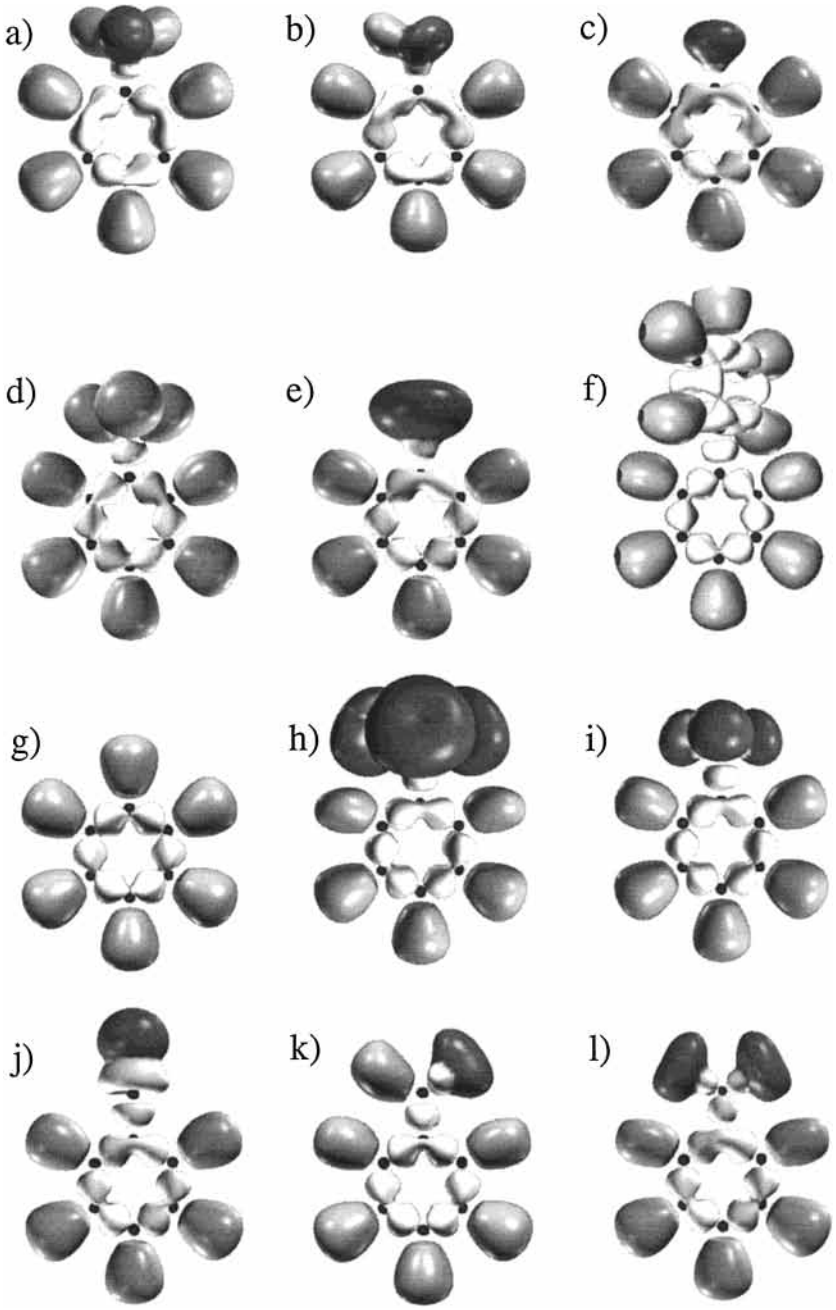

Figure 3. $\eta = 0.65$ localization domains of monosubstituted benzenes: (a) $C_6H_5NH_2$, (b) C_6H_5OH, (c) C_6H_5F, (d) $C_6H_5CH_3$, (e) C_6H_5Cl, (f) C_6H_5-C_6H_5, (g) C_6H_6, (h) $C_6H_5CCl_3$, (i) $C_6H_5CF_3$, (j) C_6H_5CN, (k) C_6H_5CHO, (l) $C_6H_5NO_2$. This figure, presented here in black and white, is available in color on the World Wide Web in Supporting Information. Color code: magenta = core, red = valence monosynaptic, green = valence disynaptic.

hierarchy of splittings which can be visualized as a bifurcation tree diagram, as displayed for the benzene of Figure 1.

In Figure 2A,B,C are reported the ELF isosurfaces for $\eta(r) = 0.5, 0.6, 0.65$, respectively. The complete topology of benzene might be displayed upon progressive variation of ELF. For a low value of ELF, ≤ 0.5 (Figure 2A), one gets a contour which only reveals the 6-fold shape, all domains being fused. At ELF = 0.6 (Figure 2B), the preceding bulk volume has split, at critical ELF = 0.58 value, into six $V(C_i, H_i)_{i=1,6}$ protonated domains and a distorted toroidal volume which is typical of aromaticity. In coming discussions, it will be referred to as "aromatic domain". In turn, the aromatic domain splits into six distinct $V(C_i, C_{i+1})_{i=1,5}$ and $V(C_1, C_6)$ domains at the critical ELF value of 0.6449, as displayed in Figure 2C. The latter value of ELF will be used for the sake of comparison when dealing with substituted compounds. This progressive splitting of the various domains yields the bifurcation diagram of Figure 1, which summarizes the various preceding steps.

The analysis of a bifurcation diagram brings interesting information about the electron localization on the various sites of a given aromatic compound. Indeed, electronic pairing is more pronounced around a site bearing some negative charge. Consequently, the corresponding localization domains appear at larger ELF values than for their related less negative counterparts. Thus, the bifurcation diagram distinguishes the preferential sites of electrophilic attack as these which separate at highest ELF values.

4. Monosubstituted Benzene Derivatives

Figure 3 displays the localization domains bounded by the $\eta(\mathbf{r}) = 0.650$ isosurface of benzene and 11 monosubstituted derivatives C_6H_5-S. For the sake of the analysis it is useful to

TABLE 1: Calculated Electrophilic Substitution Positional Indices of Monosubsituted Benzenes

	6-31G**/HF			6-31G**/Becke3LYP		
S	*ortho*	*meta*	*para*	*ortho*	*meta*	*para*
NH_2	0.042	−0.021	0.029	0.039	−0.017	0.024
OH	0.035	−0.019	0.024	0.030	−0.012	0.018
F	0.024	−0.012	0.011	0.019	−0.006	0.009
CH_3	0.013	−0.007	0.010	0.016	−0.004	0.006
C_6H_5	0.007	−0.004	0.009	0.009	−0.002	0.004
Cl	0.004	−0.004	0.001	0.008	−0.001	0.002
H	0.0	0.0	0.0	0.0	0.0	0.0
CCl_3	−0.009	0.001	−0.011	−0.003	0.0	−0.004
CF_3	−0.009	0.001	−0.011	−0.008	0.001	−0.006
CN	−0.016	0.003	−0.016	−0.010	0.002	−0.009
CHO	−0.018	0.008	−0.017	−0.020	0.004	−0.011
NO_2	−0.032	0.009	−0.025	−0.030	0.006	−0.015

partition the molecular space in two parts: on one hand, the subspace formed by the basins which only belong to the substituent S and, on the other hand, the remaining space involving the phenyl group basins. The V(C, S) disynaptic basin linking the substituent to the phenyl skeleton belongs to the latter subspace. In the phenyl subspace the number and the type of the basin are identical, therefore all the ELF gradient fields are isomorphic. This means that the ELF gradient field within the phenyl subspace is structurally stable with respect to the substitution which can be consequently considered as a weak perturbation. Moreover, the isomorphism implies that the critical points located in the phenyl subspace are topological invariants.

The phenyl group localization domains as displayed in Figure 3 show two kinds of bifurcation diagram according to the nature of the substituent. For *ortho*−*para* orienting substituents, namely S = NH_2, OH, F, Cl, CH_3, and C_6H_5, the first splitting of the aromatic domain occurs at the level of the carbons in *meta* position whereas for *meta* orienting substituents as S = CCl_3, CF_3, CN, CHO, and NO_2 it occurs at the level of the *ortho* and *para* carbons. From a qualitative point of view, the graphical representation clearly indicates which carbons are the reactive sites. In turn, the information provided by Figure 3 can be expressed in terms of numbers by considering the values $\eta(C_i; S)$ of the localization function at the (3, −1) critical points located on the separatrices of the $V(C_{i-1}, C_i)$ and $V(C_i, C_{i+1})$ basins of the S-substituted derivative. These values rule the bifurcation diagram of the aromatic domain and are expected to enable a quantitative comparison of the effects of the substituents. Instead of the $\eta(C_i)$ themselves it is more convenient to introduce electrophilic substitution positional indices defined as

$$RI_c(S) = \eta(C_i; S) - \eta(C_i; H) \quad (4)$$

in which the subscript *c* denotes the position of the carbon labeled by *i*, i.e., *ortho*, *meta*, or *para*. The electrophilic substitution positional index is just the difference of the ELF values at equivalent topological invariants in the S-derivative and in benzene. They are local measures of the perturbation of the electron localization function by the substituent.

The electrophilic substitution positional indices calculated at the 6-31G**/HF and Becke3LYP levels are listed in Table 1. As a general rule, for a given species the *ortho* and *para* indices have the same sign and the *meta* index has the opposite sign. A positive index betokens a favored electrophilic substitution position. Though there are differences between the Hartree−Fock and Becke3LYP values for corresponding indices, the two approaches yield the same order with respect to the nature of the substituent. The chemical interpretation of the electrophilic substitution positional indices follows a remark which can be made by examining the substituent localization domains of the substituents in Figure 3. The cores of the most electronegative atoms are always surrounded by a single reducible localization domain which reproduces the atomic valence shell. Of course, this domain gives rise to irreducible localization domains at higher values of the ELF function. The larger the electronegativity, the higher will be the ELF value enabling the corresponding splitting of the domain. The ELF value at the (3, −1) critical point corresponding to the complete reduction of localization around a given center is a measure of its electronegativity. The electrophilic substitution positional indices are therefore related to the in situ electronegativity of the carbons.

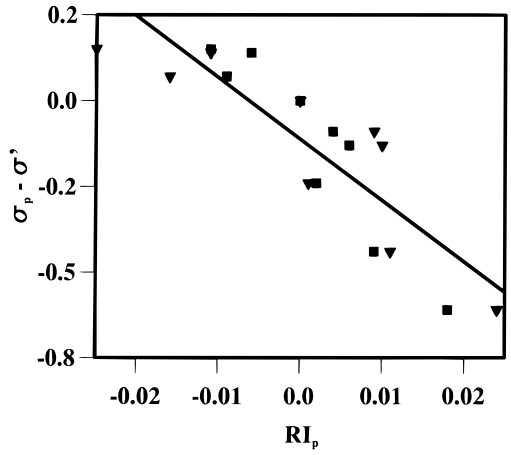

Figure 4. $\sigma_{para} - \sigma'$ vs $RI_{para}(S)$: ■ Hartree−Fock, ▼ Becke3LYP.

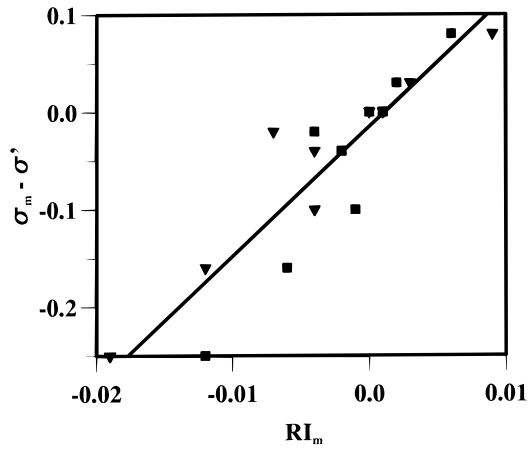

Figure 5. $\sigma_{meta} - \sigma'$ vs $RI_{meta}(S)$: ■ Hartree−Fock, ▼ Becke3LYP.

The effect of substituent on *meta* and *para* electrophilic substitutions has been phenomenologically rationalized by the Hammett equation[48] which expresses the rates or the equilibria in terms of two parameters, σ and ρ. The former characterizes the substituent and the site where the reaction takes place; the latter depends upon the nature of the reaction and the conditions. The values of σ which account for the reactivity of the *para* and *meta* positions hamper its direct use to establish a positional hierarchy of the substituents; for example, though NH_2 and F are both *para*-director, their σ_{para} constants have opposite signs because the substitution is easier for aniline than for fluorobenzene. This difficulty can be removed either by considering the differences ($\sigma_{meta} - \sigma_{para}$) or by the introduction of the so-called polar substituent constant σ' [49] which is used to form ($\sigma_{para} - \sigma'$) and ($\sigma_{meta} - \sigma'$). Figures 4 and 5 compare our reactivity indices RI_{para} and RI_{meta} to these latter differences. A rather satisfactory linear correlation is observed which enables the

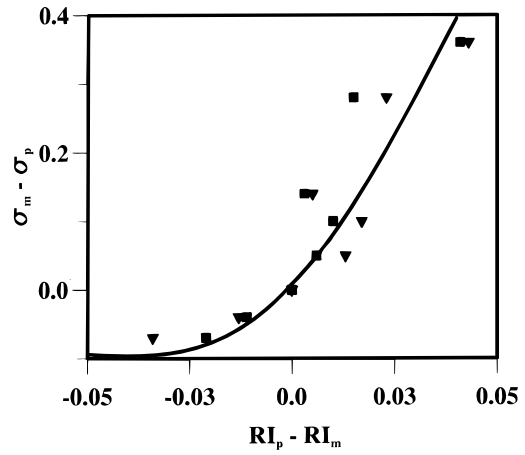

Figure 6. $\sigma_{meta} - \sigma_{para}$ vs $RI_{para}(S) - RI_{meta}(S)$: ■ Hartree−Fock, ▼ Becke3LYP.

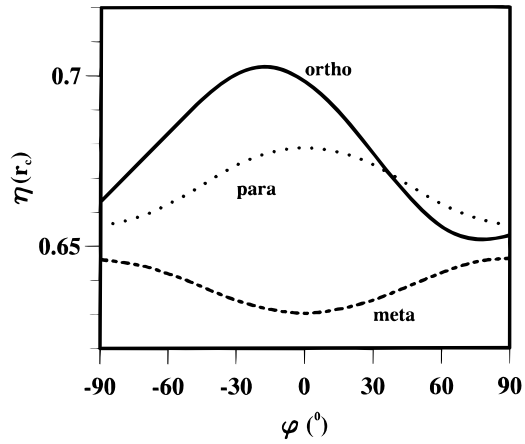

Figure 7. Angular dependence $\eta(C_i)$ vs φ for aniline: full line, *ortho*; dashed line, *para*; dotted line, *meta*.

proposal of the following approximate relationships:

$$\sigma_{para} - \sigma' \approx -40.2RI_{para} \quad (5)$$

$$\sigma_{meta} - \sigma' \approx -17.8RI_{para} \quad (6)$$

Finally, the behavior of ($\sigma_{para} - \sigma_{meta}$) with respect to ($RI_{para} - RI_{meta}$), Figure 6, looks very similar to the rate constant curves of the solvolysis of aryl−propyl tosylates discussed by Raber et al.[50]

In the standard molecular orbital framework, the substituent effect is the sum of two contributions, one arising from the π-system the other from σ-orbitals. In our approach, valence basin contributions are considered instead of molecular orbital contributions. The importance of the lone pair basin of the substituent can be discussed in the case of aniline which has one lone pair borne by the nitrogen atom. Figure 7 shows the variation of $\eta(C_i)$ for the *ortho*, *meta*, and *para* position as a function of the dihedral angle φ made by the plane containing the C−N bond and the V(N) attractor with a plane perpendicular to the ring. The three curves have a periodicity of 180°. The *para* and *meta* curves have their maximal amplitudes at $\varphi = 0°$ whereas as the two *ortho* positions are not equivalent because the maxima are at $\varphi \sim \pm 10°$. The decomposition in terms of even powers of cos φ shows that the *meta* and *para* curves behave essentially as $\cos^2 \varphi$ and the *ortho* one as $\cos^4(\varphi + 10)$. This different behavior of the *ortho* $\eta(C_i)$ and therefore of

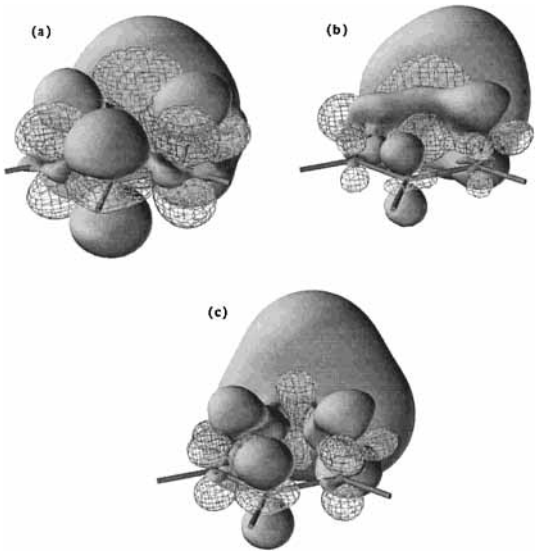

Figure 8. Deformation electron density isosurfaces $\Delta\rho = \pm 0.0005$. Full volume electron density gain, wire frame electron density loss: (a) aniline $\varphi = 0.0$, (b) aniline $\varphi = 90.0$, (c) toluene. This figure, presented here in black and white, is available in color on the World Wide Web in Supporting Information.

RI_{ortho} might be among the causes of the breakdown of the Hammett equation for *ortho* substitution. In the case of aniline the V(N) contribution appears to be the dominant one at the equilibrium geometry ($\varphi = 0°$), that due to the V(C, N) basin being very weak. In the case of toluene, the $\eta(C_i)$ are independent of the rotation of the methyl group. This follows from the specific forms of the $\eta(C_i)$'s independently of the strength of the hyperconjugacy:

$$\cos^2 \varphi + \cos^2(\varphi + 120) + \cos^2(\varphi - 120) = {}^3/_2 \quad (7)$$

$$\cos^4 \varphi + \cos^4(\varphi + 120) + \cos^4(\varphi - 120) = {}^9/_4 \quad (8)$$

The electron transfers between the substituent and the phenyl group are evidenced by the electron density deformation ($\rho(C_6H_5S) - \rho(C_6H_6)$). Figure 8 displays the isosurfaces $\Delta\rho = \pm 0.0005$ e^- $bohr^{-3}$ for aniline ($\varphi = 0$, 90.0) and for toluene. For aniline the largest transfers occur at $\varphi = 0$. As expected from molecular orbital theory arguments it mostly involves the π-system with losses on the *meta* carbons and gains on the *ortho* and *para* ones. Each corresponding isosurface is made of two lobes centered on a carbon which strongly suggests the density of the $2p_z$ atomic orbital. The σ-transfer is weaker and in phase opposition: gains in *meta*, losses in *ortho*−*para*. When the lone pair axis is in the ring plane, the size of all lobes is decreased with respect to the $\varphi = 0$ situation. The remaining π-transfers are due to hyperconjugacy whereas the weakening of the σ one might be due to the participation of the lone pair. The toluene case unequivocally illustrates the hyperconjugacy effect.

5. Polysubstituted and Polyaromatic Derivatives

In the previous section it has been shown that the substitution of a hydrogen by another functional group weakly perturbs the localization gradient field of the phenyl group. The electrophilic substitution positional indices are the linear response coefficient of the ELF function at the (3, −1) critical points of the aromatic domain. The addition of another substituent is expected to also be a weak perturbation for which the linear response approximation holds. The reactivity indices of a polysubstituted

TABLE 2: Calculated and Estimated Electrophilic Substitution Positional Indices of Polysubstituted Benzenes

molecule	c_1	c_2	S_1	S_2	calc	est
o-$C_6H_4F_2$	*meta*	*ortho*	F	F	0.012	0.013
	meta	*para*	F	F	0.003	0.003
	para	*meta*	F	F	0.003	0.003
	ortho	*meta*	F	F	0.012	0.013
m-$C_6H_4F_2$	*ortho*	*ortho*	F	F	0.039	0.038
	para	*ortho*	F	F	0.028	0.028
	meta	*meta*	F	F	−0.012	−0.012
	ortho	*para*	F	F	0.028	0.028
p-$C_6H_4F_2$	*ortho*	*meta*	F	F	0.013	0.013
m-$C_6H_4(CH_3)_2$	*ortho*	*ortho*	CH_3	CH_3	0.027	0.026
	ortho	*para*	CH_3	CH_3	0.023	0.023
	meta	*meta*	CH_3	CH_3	−0.013	−0.014
	para	*ortho*	CH_3	CH_3	0.023	0.023
o-C_6H_4OHCl	*ortho*	*meta*	OH	Cl	0.029	0.031
	meta	*para*	OH	Cl	−0.020	−0.018
	meta	*ortho*	OH	Cl	−0.015	−0.015
	para	*meta*	OH	Cl	0.021	0.020

TABLE 3: Value of the ELF Function at the (3, −1) Critical Points of the Aromatic Domains of the Naphthalene and Anthracene Molecules

position	naphthalene	anthracene
C_3	0.6704	0.6836
C_4	0.6674	
C_5	0.6674	0.6691
C_6	0.6704	0.6650

benzene should therefore be a sum of monosubstituted derivative indices:

$$RI_{c_1,c_2,...}(S_1,S_2,...) \approx RI_{c_1}(S_1) + RI_{c_2}(S_2) + ... \qquad (9)$$

The notation is consistent with that used eq 4 for monosubstituted derivatives: the successive c_i indices are the positions with respect to the successive substituents S_i. The additivity of the electrophilic substitution positional indices has been verified on the three difluoro-benzene isomers, on the *meta* dimethyl benzene, and on the *ortho* chloro phenol. Table 2 compares the electrophilic substitution positional indices of these molecules explicitly calculated on the disubstituted molecules themselves and estimated by eq 9 with the values of Table 1. There is an excellent agreement between the two series of values. The additivity of the electrophilic substitution positional indices is consistent with the correlation with the Hammett constants since these latter are also additive.

The generalization of the method to polyaromatic molecules is straightforward. The carbon labels of naphthalene and anthracene are as follows:

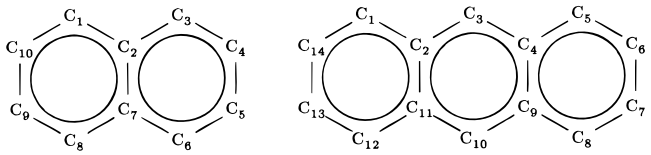

The ELF values at the (3, −1) critical points of the aromatic domains are listed in Table 3. In agreement with experiment, the electrophilic substitution center of naphthalene is the carbon C_3. Each cycle of the naphthalene can be considered as a disubstituted benzene on the carbon C_1 and C_6; however, eq 9 cannot legitimately be applied to estimate the ELF values at the critical points because their deviations from the benzene value are a sum of two contributions: one arising from the other cycle which is accounted for by the electrophilic substitution positional indices, the other one being due to the fact that each cycle itself acts as a substituent. Nonetheless, a qualitative reasoning holds. The values of Table 1 show that for *ortho*/*para* director substituents, the *ortho* electrophilic substitution positional index has always the largest absolute value. For the C_3 carbon the total contribution of the other cycle is of the form $RI_{ortho} + RI_{meta}$ and larger than that of C_4, namely $RI_{para} + RI_{meta}$. The same arguments hold to explain why C_3 is also the reactive center in anthracene.

TABLE 4: Additivity of the Electrophilic Substitution Positional Indices of Fluoro Naphthalenes

			1,4-$C_{10}H_6F_2$	
position	1-$C_{10}H_7F$	4-$C_{10}H_7F$	calc	est
C_1		0.002		
C_3	−0.007	0.026	0.020	0.019
C_4	−0.001			
C_5	−0.003	0.012	0.010	0.009
C_6	−0.001	−0.005	−0.006	−0.006
C_8	0.005	−0.002	0.003	0.003
C_9	−0.005	0.001	−0.004	−0.004
C_{10}	0.024	−0.004	0.027	0.020

For substituted and polysubstituted polyaromatic molecules it is convenient to generalize the electrophilic substitution positional index concept. The definition is the same as previously cited (see eq 4), the $\eta(C_i; H)$ being the values of the hydrogenated compound. Table 4 reports the calculated values of these indices for the 1- and 4-fluoro naphthalenes and for the 1,4-difluoro naphthalene. In the monosubstituted molecules, the largest indices correspond to the *ortho*-like position within a cycle; they are of the same order of magnitude as fluoro benzene: slightly larger in 1-fluoro naphthalene in which there is only one *ortho*-like position whereas in 4-fluoro naphthalene the average of the two *ortho*-like indices is the *ortho* value of fluoro benzene. The transferability of the fluoro-benzene indices to fluoro naphthalene is very good for the *meta* positions. The fulfillment of the additivity property is verified by the estimated values given in the last column of Table 4.

6. Conclusion

The results presented in this report show that the topological analysis of the electron localization function is a sound basis for the determination of the electrophilic substitution site and, more generally, for the localization of the reactive sites in molecules. The ELF analysis provides ready-for-use qualitative visual information through the graphical representation of the localization domains. Quantitatively, the electrophilic substitution positional indices make a link between the results of the calculation and the Hammett constants. As these latter, they are additive, which makes possible reliable predictions on a large number of polysubstituted derivatives without explicit calculations of their wave functions. This method complements the description of the reactivity already provided by the frontier orbital and the atoms in molecules theories. The use of the ELF function emphasizes the importance of the local Pauli repulsion as a token of local electronegativity.

Acknowledgment. The authors gratefully acknowledge Prof. J. Molina's comments on the draft manuscript. The data analyzer software SciAn[51] has been used to produce Figures 2, 3, and 8.

Supporting Information Available: The color version of Figures 2, 3, and 8. This material is available free of charge via the Internet at http://pubs.acs.org.

References and Notes

(1) Holleman, A. F. *Rec. Trav. Chim. Pays-Bas* **1906**, *24*, 140.
(2) Holleman, A. F. *Chem. Rev.* **1925**, *1*, 187.

(3) Holleman, A. F.; Wibaut, J. P. *Organic Chemistry, a translation from the sixteenth deutch edition*; Elsevier: Amsterdam, 1951.
(4) Norman, R. O. C. *Electrophilic substitution in Benzenoid compounds*; Elsevier: Amsterdam, 1965.
(5) Hückel, E. *Z. Phys.* **1931**, *70*, 204.
(6) Hückel, E. *Z. Phys.* **1931**, *72*, 310.
(7) Hückel, E. *Z. Phys.* **1932**, *76*, 628.
(8) Wheland, G. W. *Resonance in Organic Chemistry*; Wiley: New York, 1955.
(9) Ingold, C. K. *Structure and Mechanisms in Organic Chemistry*; Bell and Sons: London, 1953.
(10) Coulson, C. A. *Valence*; Clarendon: Oxford, 1952.
(11) Streitweiser, A., Jr. *Molecular Orbital Theory for Organic Chemists*; Wiley: New York, 1961.
(12) Salem, L. *The Molecular Orbital Theory of Conjugated Systems*; W. A. Benjamin Inc.: Reading, 1966.
(13) Dewar, M. J. S. *The Molecular Orbital Theory of Organic Chemistry*; McGraw-Hill: New York, 1968.
(14) Epiotis, N. D. *J. Am. Chem. Soc.* **1973**, *95*, 3188.
(15) Epiotis, N. D.; Cherry, W. *J. Am. Chem. Soc.* **1976**, *98*, 4361.
(16) Epiotis, N. D.; Cherry, W. *J. Am. Chem. Soc.* **1976**, *98*, 4365.
(17) Epiotis, N. D.; Cherry, W. *J. Am. Chem. Soc.* **1976**, *98*, 5432.
(18) Bader, R. F. W. *Atoms in Molecules: A Quantum Theory*; Oxford Univ. Press: Oxford, 1990.
(19) Bader, R. F. W.; Chang, C. *J. Phys. Chem.* **1989**, *93*, 2946.
(20) Bader, R. F. W.; Chang, C. *J. Phys. Chem.* **1989**, *93*, 5095.
(21) Cubero, E.; Orozco, M.; Luque, F. J. *J. Phys. Chem. A* **1999**, *103*, 315.
(22) Becke, A. D.; Edgecombe, K. E. *J. Chem. Phys.* **1990**, *92*, 5397.
(23) Savin, A.; Becke, A. D.; Flad, J.; Nesper, R.; Preuss, H.; von Schnering, H. G. *Angew. Chem., Int. Ed. Engl.* **1991**, *30*, 409.
(24) Savin, A.; Jepsen, O.; Flad, J.; Andersen, O. K.; Preuss, H.; von Schnering, H. G. *Angew. Chem., Int. Ed. Engl.* **1992**, *31*, 187.
(25) Silvi, B.; Savin, A. *Nature* **1994**, *371*, 683.
(26) Savin, A.; Silvi, B.; Colonna, F. *Can. J. Chem.* **1996**, *74*, 1088.
(27) Savin, A.; Nesper, R.; Wengert, S.; Fässler, T. F. *Angew. Chem., Int. Ed. Engl.* **1997**, *36*, 1809.
(28) Noury, S.; Colonna, F.; Savin, A.; Silvi, B. *J. Mol. Struct.* **1998**, *450*, 59.
(29) Hehre, W. J.; Ditchfield, R.; Pople, J. A. *J. Chem. Phys.* **1972**, *56*, 2257.
(30) Clark, T.; Chandrasekhar, J.; Spitznagel, G. W.; Schleyer, P. v. R. *J. Comput. Chem.* **1983**, *4*, 294.
(31) Frisch, M. J.; Pople, J. A.; Binkley, J. S. *J. Chem. Phys.* **1984**, *80*, 3265.
(32) Becke, A. D. *J. Chem. Phys.* **1993**, *98*, 5648.
(33) Becke, A. D. *Phys. Rev.* **1988**, *A38*, 3098.
(34) Lee, C.; Yang, Y.; Parr, R. G. *Phys. Rev.* **1988**, *B37*, 785.
(35) Miechlich, B.; Savin, A.; Stoll, H.; Preuss, H. *Chem. Phys. Lett.* **1989**, *157*, 200.
(36) Frisch, M. J.; Trucks, G. W.; Schlegel, H. B.; Gill, P. M. W.; Johnson, B. G.; Robb, M. A.; Cheeseman, J. R.; Keith, T.; Petersson, G. A.; Montgomery, J. A.; Raghavachari, K.; Al-Laham, M. A.; Zakrzewski, V. G.; Ortiz, J. V.; Foresman, J. B.; Cioslowski, J.; Stefanov, B. B.; Nanayakkara, A.; Challacombe, M.; Peng, C. Y.; Ayala, P. Y.; Chen, W.; Wong, M. W.; Andres, J. L.; Replogle, E. S.; Gomperts, R.; Martin, R. L.; Fox, D. J.; Binkley, J. S.; Defrees, D. J.; Baker, J.; Stewart, J. P.; Head-Gordon, M.; Gonzalez, C.; Pople, J. A. *Gaussian 94, Revision D.4*; Gaussian Inc.: Pittsburgh, PA, 1995.
(37) Alikhani, M. E.; Bouteiller, Y.; Silvi, B. *J. Phys. Chem.* **1996**, *100*, 16092.
(38) Fourré, I.; Silvi, B.; Chaquin, P.; Sevin, A. *J. Comput. Chem.* **1999**, *20*, 897.
(39) Llusar, R.; Beltrán, A.; Andrés, J.; Noury, S.; Silvi, B. *J. Comput. Chem.* **1999**, *20*, 1517.
(40) Beltrán, A.; Andrés, J.; Noury, S.; Silvi, B. *J. Phys. Chem. A* **1999**, *103*, 3078.
(41) Berski, S.; Silvi, B.; Latajka, Z.; Leszczynski, J. *J. Chem. Phys.* **1999**, *111*, 2542.
(42) Krokidis, X.; Noury, S.; Silvi, B. *J. Phys. Chem. A* **1997**, *101*, 7277.
(43) Krokidis, X.; Goncalves, V.; Savin, A.; Silvi, B. *J. Phys. Chem. A* **1998**, *102*, 5065.
(44) Krokidis, X.; Silvi, B.; Alikhani, M. E. *Chem. Phys. Lett.* **1998**, *292*, 35.
(45) Krokidis, X.; Vuilleumier, R.; Borgis, D.; Silvi, B. *Mol. Phys.* **1999**, *96*, 265.
(46) Noury, S.; Krokidis, X.; Fuster, F.; Silvi, B. *Topmod package*, 1997.
(47) von Weizsácker, C. F. *Z. Phys.* **1935**, *96*, 431.
(48) Hammett, L. P. *Chem. Rev.* **1935**, *35*, 125.
(49) Roberts, J. D.; Moreland, W. T. *J. Am. Chem. Soc.* **1953**, *75*, 2167.
(50) Raber, D. J.; Harris, J. M.; Schleyer, P. v. R. *J. Am. Chem. Soc.* **1971**, *93*, 4829.
(51) Pepke, E.; Murray, J.; Lyons, J.; Hwu, T.-Z. *Scian*; Supercomputer Computations Research Institute; Florida State University: Tallahassee, FL, 1993.